2D Positional profiling of orientation and thickness uniformity in the semiconducting polymers thin films

Nikita Kumari,[a,*] Atul S. M. Tripathi,[a] Sadakata Shifumi,[a] Manish Pandey,[a] Shuichi Nagamatsu,[b] Shuzi Hayase,[a] Shyam S. Pandey,[a,**]

[a]Division of Green Electronics, Graduate School of Life Science and Systems Engineering, Kyushu Institute of Technology, Wakamatsu, Kitakyushu, 808-0196 Japan

[b]Department of Computer Science and Electronics, Kyushu Institute of Technology, Iizuka, 820-2502 Japan

Corresponding Author
*Nikita Kumari (nikita.jisce@gmail.com)
**Prof. Shyam S. Pandey (shyam@life.kyutech.ac.jp)

Keywords: 2D positional Mapping; large area characterization; molecular orientation; conjugated polymer; polarized absorption spectra; Floating Film Transfer.

Abstract: Harnessing the full potential of solution processable conjugated polymers (CPs) as active semiconductor elements lies in the facile thin film fabrication along with amicable control of molecular self-assembly and orientation. Probing the nature and uniformity of thin films are inevitable for fabrication of devices with high reproducibility. Herein, a new method for the fast and facile profiling of thickness and molecular orientation of large area thin films is being reported. Thin films of PBTTT-C14 fabricated by three different methods like floating film transfer method (FTM), friction transfer and spin coating were subjected to profiling of thickness and molecular orientation using 2D positional mapping system followed by fabrication of organic thin film transistors. In order to prove applicability of the mapping system on other CPs, oriented films of PQT-C12 were also prepared by FTM and optical anisotropy estimated by the mapping system (23.0) and conventional spectrophotometer (22.4) validates the performance of our positional mapping system. Spin-coated thin films of PBTTT-C14 subjected to positional profiling of the film uniformity revealed that films are non-uniform and there was a gradual increase in the thickness from center to the periphery.

1. Introduction: Organic semiconducting materials have drawn widespread attention in the recent past due to their vital application in diverse areas of flexible, wearable and transparent electronics [1–3]. Advent of solution processable organic semiconductors diversified the field of organic electronics owing to their potential applications in the area of organic field effect transistors (OFETs), organic light-emitting diodes, organic memristors and organic photovoltaic cells etc. [4–11]. Charge transport in organic semiconductors occurs through π-conjugated backbone assisted by the overlapping of π–electron clouds between adjacent molecules and inter-chain as well as inter-domain hopping [12-14]. Organic semiconductors are semi-crystalline in nature due to their low intermolecular interactions leading to poor charge transport compared to their inorganic counterparts [15]. In this context, small molecular semiconductors outpace polymeric semiconductors as they show high mobility due to their high crystallinity. Although there are some recent reports regarding printing compatible solution processing of molecular semiconductor, in most reports high field effect mobility (μ) in molecular semiconductors is achieved through vacuum deposition or by growing single crystalline thin films through solution processing and at the same time, the device to device μ variation is also a major issue [16–18]. On the other hand, the last decade witnessed dramatic enhancement in the μ of semiconducting polymers (SCPs) reaching > 10 $cm^2/V{\cdot}s$ [19,20]. Additional features possessed by SCPs is their high solubility in organic solvents and better solution rheology, concomitantly imparting high device uniformity, which makes them a potential candidate for printed electronics [21].

Due to quasi one-dimensional nature of SCPs, morphology of their thin films plays an important role in deciding the device performance. Especially, μ of the SCPs are expected to be enhanced dramatically by orienting the polymeric chains along the channel direction of the OEFTs and charge transport anisotropy significantly increases with respect to their extent of orientation [22–24]. In recent past, a number of techniques have been reported to orient the

SCPs, such as mechanical rubbing, friction transfer, floating film transfer method (FTM), strain-alignment, flow coating, off-center spin-coating, and solution shearing etc. [24–27]. However, intriguing challenges like large area thin film fabrication along with chemical and mechanical damages associated with layer-by-layer fabrication are needed to be solved amicably [28-30]. We have recently reported ribbon-shaped FTM as a facile and cost-effective method to fabricate large area oriented thin films, shown schematically in the **Figure 1(a)** [31,32]. In this method, a single drop of polymer solution led to the fabrication of several centimeters long and homogeneous floating films. The films can be easily stamped on any desired substrates and their characteristics can also be regulated by tuning the FTM parameters during film casting as reported earlier [32–35].

In the case of large area solution processed thin films, films thickness and morphological variations are the major obstacles leading to poor device reproducibility posing the need for precise characterization of microstructural distribution in the fabricated thin films. Several techniques such as atomic force microscopy, grazing incidence x-ray diffraction, near edge x-ray absorption fine structure spectroscopy, variable angle spectroscopic ellipsometry, polarized absorption and Raman spectroscopy etc. have been widely used to probe the molecular orientation and backbone conformation in oriented SCP films [24,36–39]. However, these characterization techniques are inefficient for precise characterization if the area of thin films extends up to several square centimeters posing the need for the development of a suitable technique for the facile and fast mapping of the variation in molecular orientation and thickness. In order to provide an amicable solution to this issue, a new method for the two-dimensional (2D) positional mapping of thickness and molecular orientation in large area thin films of SCP is being reported.

In this study, thin films of poly[2,5-bis(3-tetradecylthiophen-2-yl)thieno[3,2-b]thiophene] (PBTTT-C14) were prepared by utilizing three different kind of methods such as ribbon-shaped FTM, friction transfer method and spin-coating. These films were characterized

by our proposed 2D positional mapping system to investigate the variation in the thickness as well as molecular orientation. In this technique, thin film coated on glass was illuminated with a fixed incident beam and the transmitted beam was collected by a multichannel detector. Beauty of this technique lies in the fact that at each point simultaneous light illumination and detection in the entire selected wavelength region generate the whole absorption spectrum instantaneously and in combination with the mobile sample stage the characterization of large area sample becomes swift. On intigration, the measured absorption spectra reveal the microstructural distribution throughout the sample because the absorbance of different energy photon depends on the material characteristics as well as film morphology [40]. To verify the the precision of mapping technique, comparative analysis of the results were also carried with conventional UV-Visible electronic absorption spectroscopy.

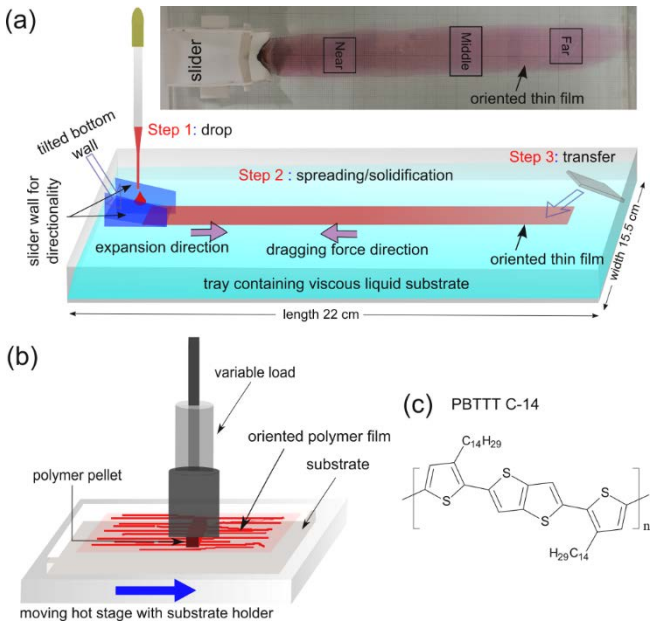

Figure 1. Schematic illustration for the mechanism of thin film fabrication by ribbon-shaped FTM along with photograph of the casted PBTTT-C14 film (a), friction transfer technique (b) and molecular structure of PBTTT-C14 (c).

2. Results and Discussion

2.1. Mapping System Operation

In order to map the thickness and molecular orientation, thin films cast on a glass substrate were mounted on the mobile stage. Absorbance of the bare substrate was measured as baseline prior to measuring the thin film cast on the same substrate. Position dependent absorption spectra were measured at varying locations through aligned light source and multichannel detector and by controlled movement of the sample stage. The sample was scanned along multiple lines to obtain the spectral distribution in the whole sample area, as illustrated in **Figure 2,** (digital image of the positional mapping system is shown in Figure S1, supporting information).

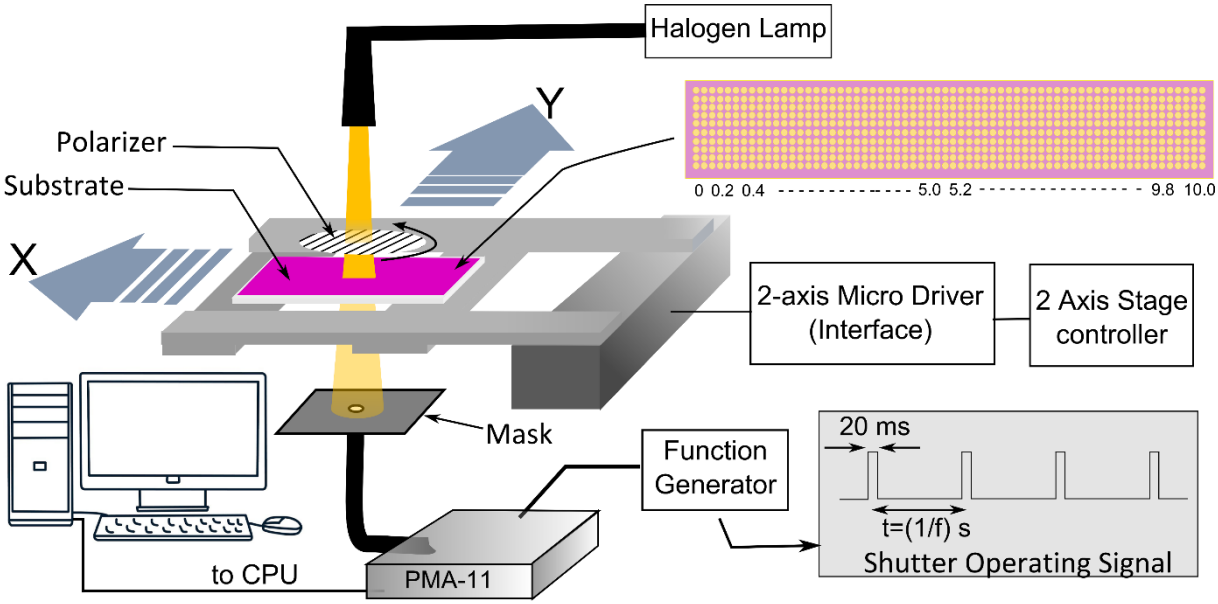

Figure 2. Schematic illustration of 2D positional mapping set-up

2D positional mapping through non-polarized and polarized electronic absorption spectra of the thin films was conducted to probe the variation of thickness and molecular orientation, respectively. In the case of polarized absorption spectra, oriented film shows higher value of absorbance when macromolecules are oriented parallel to the polarization direction of

incident light as compared to their perpendicular orientation. The extent of molecular orientation can be quantified in terms of dichroic ratio (DR), which can be calculated using the Equation 1.

$$DR = \frac{A_{\parallel}}{A_{\perp}} \quad (1)$$

Where, $A_{\parallel}$ and $A_{\perp}$ are the peak absorbance in polarized electronic absorption spectra for films oriented in parallel and perpendicular directions, respectively. To verify the results obtained by positional mapping set-up, same samples were also characterized with double beam UV-Visible spectrophotometer (JASCO V-570) equipped with Glan-Thompson prism.

2.2. Thin Film Characterization

OFETs are one of the most important components of organic electronic circuits, whose performance is controlled by nature and quality of thin films of organic semiconductors, while cost is controlled by technology being used for thin film fabrication. In this context, 2D positional mapping is expected to be a valuable tool to probe the quality of the fabricated thin film and correlate results with final device performance. In order to demonstrate this, thin films of PBTTT-C14 was taken into consideration. The non-oriented thin film of this polymer was fabricated using the most commonly used spin-coating method, while oriented films were prepared by two methods, ribbon-shaped FTM and friction transfer. Thin films of PBTTT-C14 fabricated by these three methods were then subjected to 2D positional mapping for the measurement of film uniformity and orientation along with fabrication and characterization of OFETs.

In the ribbon-shaped FTM, when a drop of polymer solution is placed at the interface of slider and orthogonal liquid substrate, walls at both edge of the slider assists unidirectional expansion of the SCP solution leading to formation of large area ribbon-shaped thin films. Quick solvent evaporation and simultaneous action of opposing viscous force during film

expansion lead to solid oriented floating film on the liquid substrate. In this work floating films of length >15 cm long along the expansion direction was fabricated on hydrophilic liquid substrate. To probe the variation in molecular orientation and thickness, three substrates (10 mm × 10 mm) were used to stamp samples from the floating films. Each sample were taken at 5 cm gap from the film at different position i.e. 1) far, 2) middle and 3) near, from the slider side as shown in Figure 1a. In order to map the thickness variation in the sample, absorption spectra measurement was performed along width direction (width of ribbon-shaped FTM film) for point areas of 3.14×10^{-2} mm^2 at an equidistant interval of 0.2 mm. The measured peak-absorbance values were correlated with the corresponding thickness values of the film using Beer-Lamberts law followed by integrating the results to show the distribution as shown in **Figure 3**. The correlation between peak-absorbance and thickness is given in supporting information, Figure S2. From the perusal of Figure 3, the resolution of the measurement can be understood. The mapped absorption spectra of collinear point-areas along width (at length = 130 mm of film) is shown in Figure 3(a)) which is further simplified in terms of location of the scanned point-areas and their corresponding peak-absorbance, Figure 3(c) and from this correlation the regional thickness variation of the actual sample was realized. This way the whole sample was mapped in discrete point areas and through integration the overall film characteristics was obtained, Figure 3 (e). For the ease of understanding this matter is also briefed under the discussion regarding mapping of spin-coated sample, forthcoming subsection.

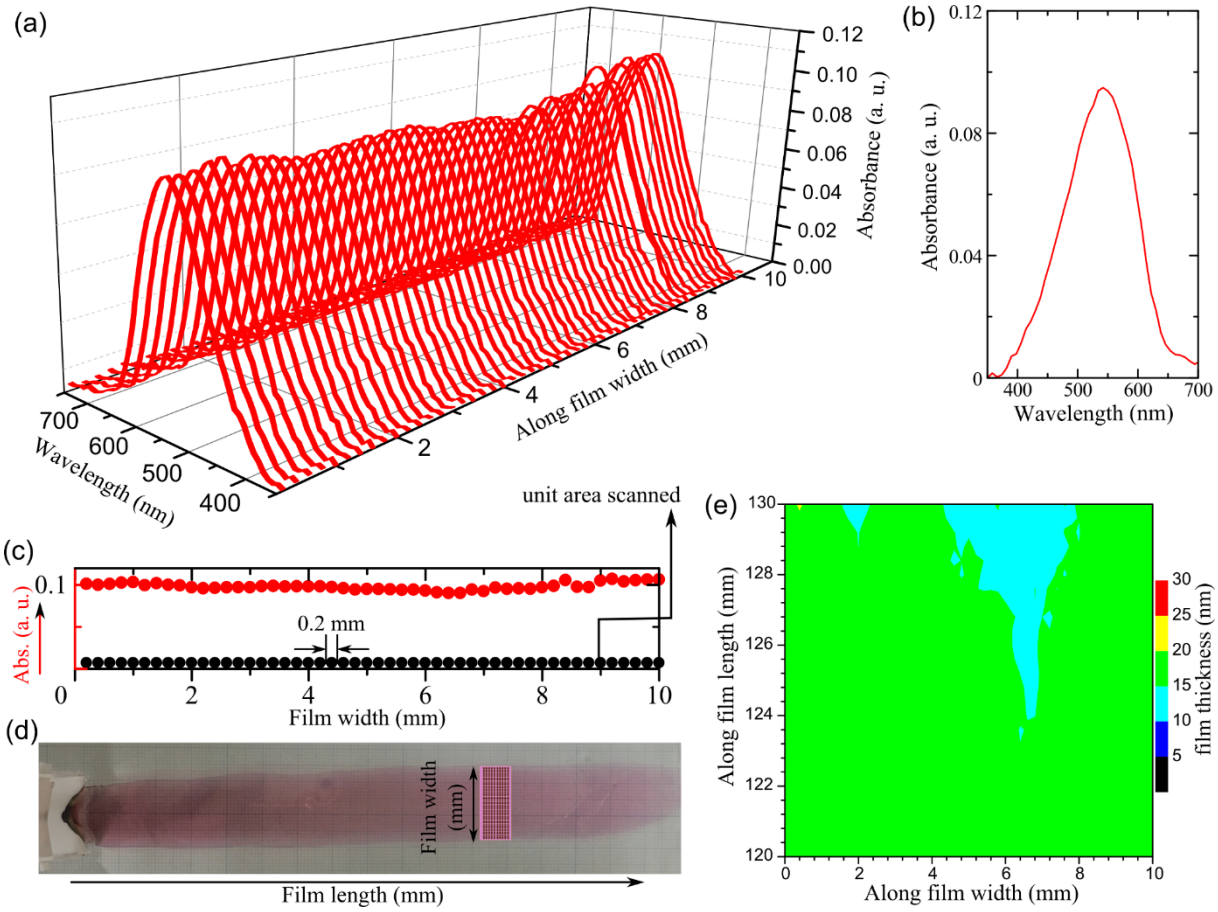

Figure 3. Absorption spectra for single line mapping of along width (at length = 130 mm) (a), absorption spectrum of the film for a single point area, 3.14 $\times 10^{-2}$ mm^2 (at length = 130 mm, width = 5 mm) (b), value of maximum absorbance corresponding to unit point area mapped along width (c), of ribbon-shaped FTM films of PBTTT (d) and mapped thickness distribution throughout the asmple (e).

Since ribbon-shaped FTM films are oriented and produce large area (≈2 cm × 15 cm), three sample specimens of 1 cm × 1 cm taken from three different regions and results obtained from the 2D positional mapping for distribution of thickness and molecular orientation is shown in **Figure 4**. It can be seen that there is uniform thickness distribution in the far-end region of the film (Figure 4a), which is due to presence of higher freedom for the film expansion. The distribution of orientation (in terms of DR) is following the opposite trend to that of thickness and thinner films exhibited relatively higher DR values (Figure 4). A perusal of profile of the entire film reveals that films are relatively uniform in the central area (Figure 4) as compared to peripheral region of the sample specimens. This can be explained considering the fact that film expands in forward direction from the slider end but it also tends to expand in the width

direction too and viscous force along the width will be more prevalent. The extent of molecular orientation in the entire FTM film was measured through conventional spectrophotometer (polarized absorption spectra shown in Figure 4 (h, i, j)), which match very well with results of 2D positional mapping system validating the accuracy of the measurement.

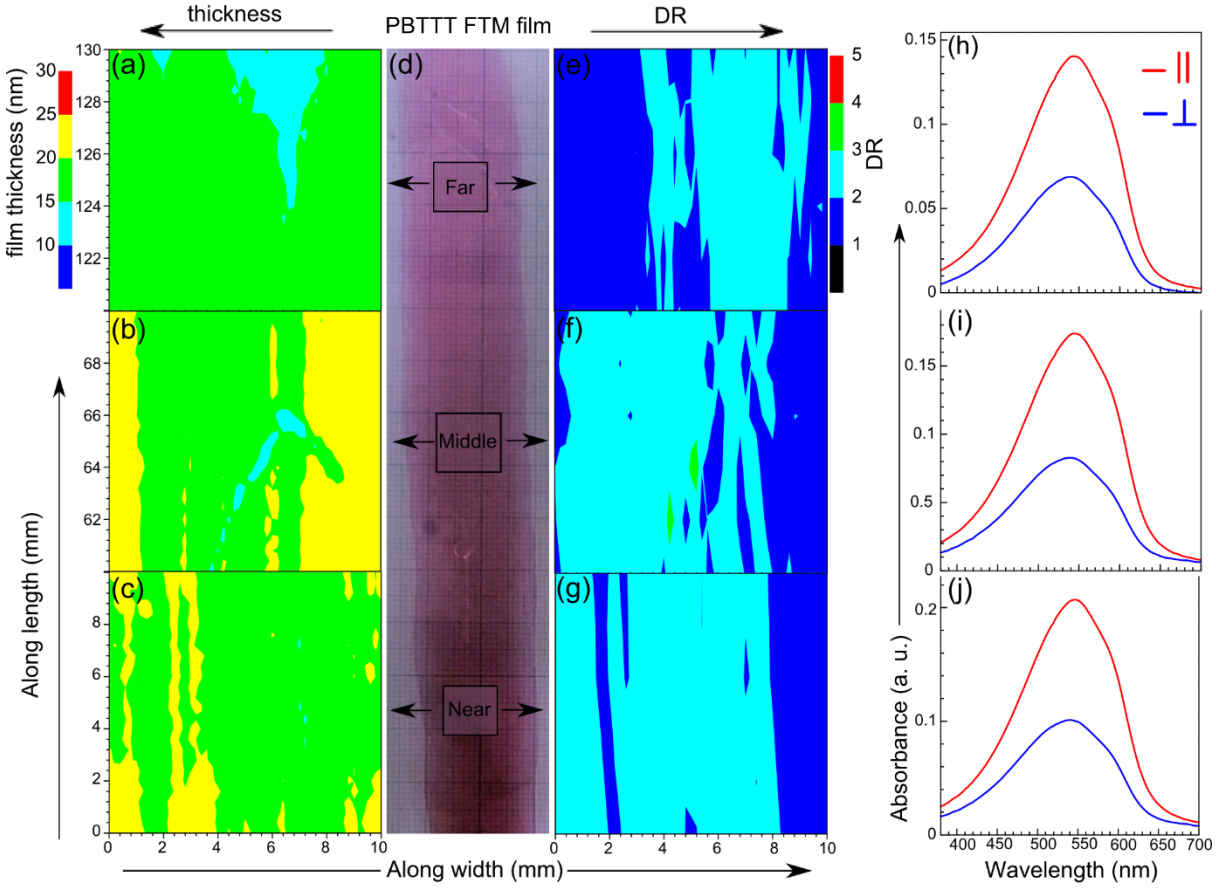

Figure 4. Mapped profiles of thickness (a-c) and orientation intensity (e-g) for the PBTTT-C14 thin films fabricated by FTM (d). Corresponding polarized electronic absorption spectra (h-j) measured by conventional spectrophotometer is shown in the extreme right.

High film uniformity in combination with molecular orientation in far-end region of the FTM films of PBTTT-C14 as probed by 2D positional mapping was used for the investigation of charge transport anisotropy in OFETs. The PBTTT-C14 films were stamped on the OTS treated Si/SiO_2 substrates. In order to obtain large ordered terrace phase morphology, films were annealed at 160 °C for 2 min and slowly cooled down to room temperature similar to work reported by Chabinyc et al. [41]. As can be seen from the output curves, OFETs exhibit clear

p-type behavior with high output current at the same gate to source voltage (V_{GS}) in the OFETs with channel parallel (||) to orientation direction in comparison to perpendicular (⊥), confirming the anisotropic charge transport (**Figure 5)**. Extracted average μ in || ($\mu_{||}$) and in ⊥ ($\mu_{\perp}$) direction, from the transfer characteristics shown in Figure 5(b) were found to be 0.12 $cm^2/V{\cdot}s$ and 0.04 $cm^2/V{\cdot}s$ respectively, with ON/OFF (I_{on}/I_{off}) ratio of ~10^6. The value $\mu_{||}/\mu_{\perp}$ of 3 is in well agreement with observed DR 2 (± 9.52%) in the as-casted films estimated by 2D positional mapping (far-end region) and conventional spectrophotometric analyses. These $\mu_{||}/\mu_{\perp}$ and DR is in well agreement as reported in detail by Lee et al. [42].

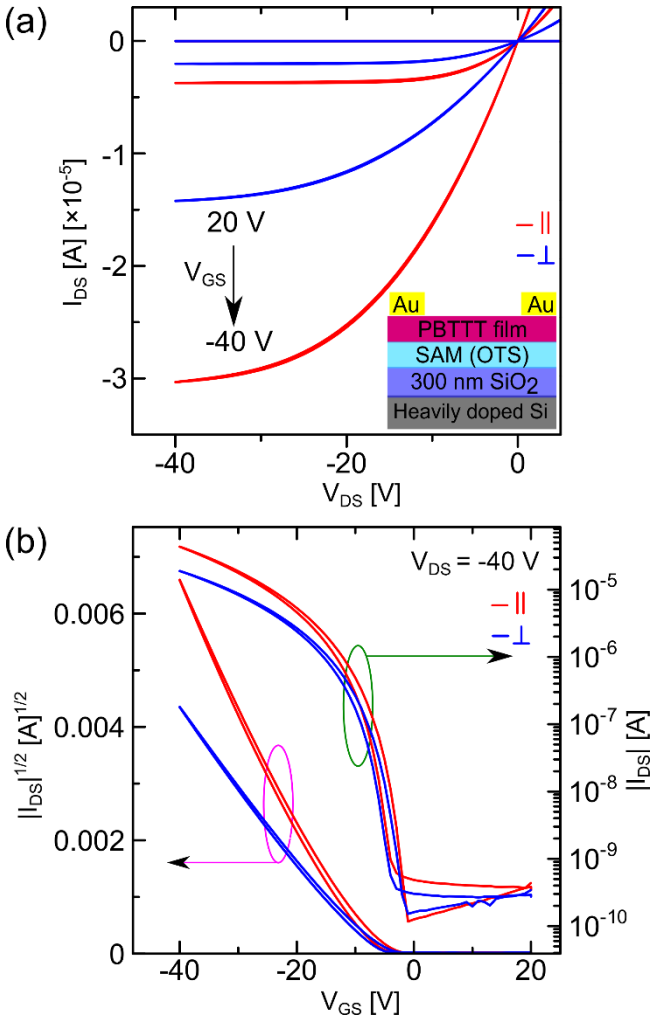

Figure 5. Output (a) and transfer (b) characteristics OFETs fabricated with far-region FTM films of PBTTT- C14 with channel direction parallel (||) and perpendicular (⊥) to the orientation direction. Inset in (a) is the schematic of fabricated OFETs.

Friction transfer method is often used to prepare oriented thin films of polymers and beauty lies in the fact that materials to be oriented are used in the form of pellet as shown in Figure 1 (b), therefore, it is applicable to insoluble SCPs also for the fabrication of oriented thin films. Although, there are reports about the attainment of very high molecular orientation and application of these films for device fabrication but details about nature of the films like uniformity in thickness and molecular orientation are not much clear [43–45]. In order to clarify this issue, oriented thin films of PBTTT-C14 was prepared on a glass substrate (1.0 cm × 2.5 cm) for 2D positional mapping of thickness and molecular orientation. Profiling of the thickness and DR was conducted along the length (drawing direction) with 0.2 mm resolution followed by same in along the width and the results are shown in the **Figure 6**.

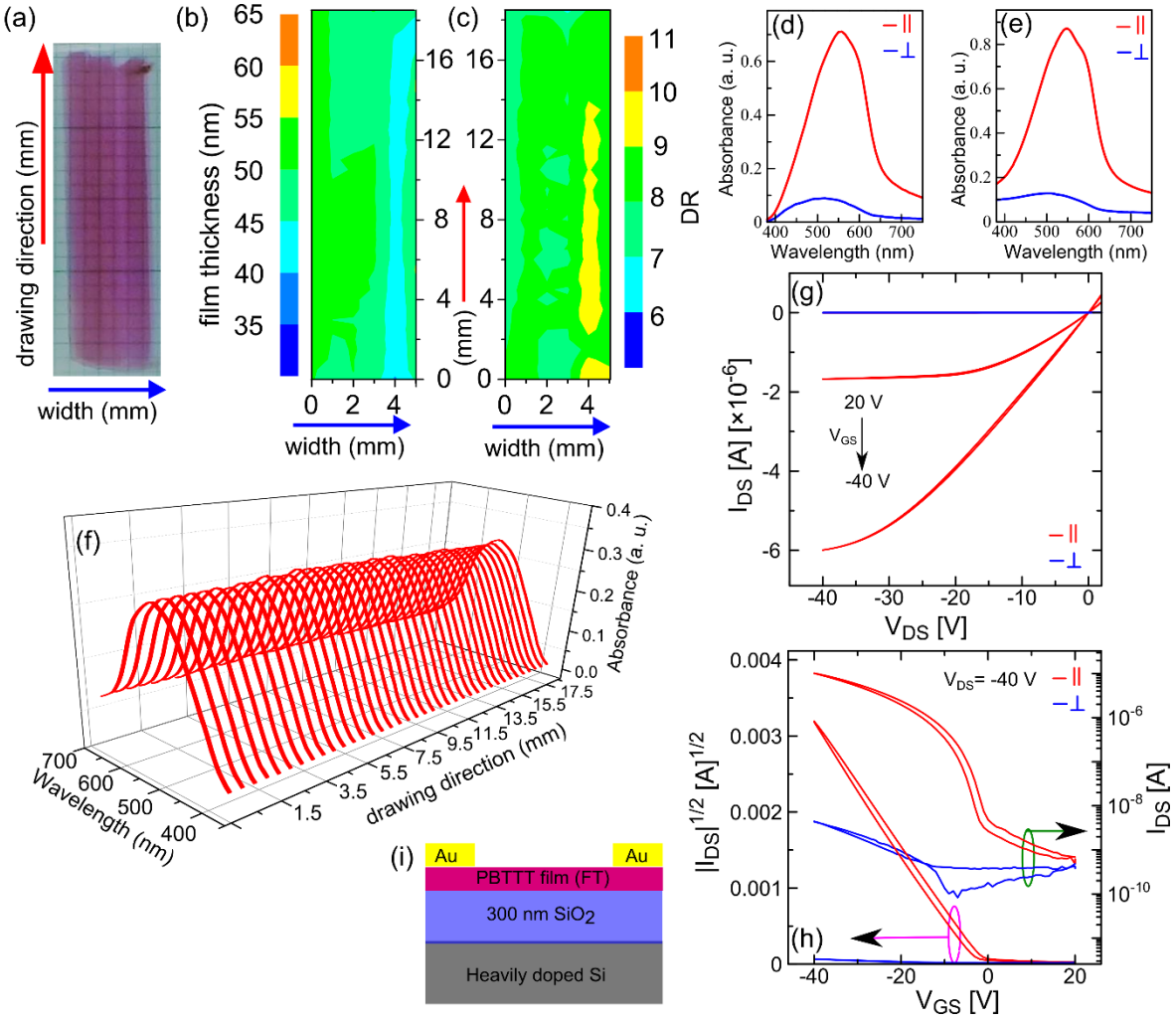

Figure 6. Digital image of the friction transferred film of PBTTT-C14 on glass (a), along with thickness distribution (b) and orientation distribution (c). Polarized absorption spectra measured by mapping technique (at a single point, 2 cm along drawing direction and width = 2 mm) (d) and conventional UV-Visible spectrophotometer (e). (f) One dimensional positional mapping of absorption spectra at width = 2 mm. Output curve (g) and transfer characteristics (h) for OFETs (i) fabricated with friction transferred thin film of PBTTT-C14.

It can be seen from this figure that films fabricated by this method possess high uniformity having an average thickness of 48.97 nm (± 7.19%) with very small variation in the thickness along the length or drawing direction (Figure 6). Some small variations in the thickness along the width direction could be attributed to the interfacial non-uniformity between the pellet and the substrate. The mapped average DR value of PBTTT-C14 films was found to be much higher 8.2 (± 7.22%) as compared to that fabricated by FTM with DR of 2 (± 9.52%). The polarized absorption spectrum at one point (near central region) probed by the mapping system (Figure 6(d)) was also compared with that measured by the conventional spectrophotometer (Figure 6(e)) and the observed optical anisotropies were almost the same (7.95 and 7.66).

OFETs were fabricated using friction transferred oriented thin films to investigate the anisotropic charge transport. It is worth to mention here that OFETs for friction transferred PBTTT-C14 films were fabricated on bare SiO_2 surface since the films do not stick well while drawing it on hydrophobic surface. However, films were annealed to obtain the terrace phase morphology as explained earlier. The observed current was extremely high in the output and transfer characteristics with orientation || to the channel direction in comparison to the ⊥ orientation as shown in Figure 6(g and h). Extracted average $\mu_{\parallel}$ and $\mu_{\perp}$ from the transfer characteristics was found to be 1.8×10^{-2} and 9.8×10^{-6} $cm^2/V{\cdot}s$ with the value of $\mu_{\parallel}/\mu_{\perp}$ in the order of 10^4. This result poses several intriguing questions like why $\mu_{\parallel}$ is so less in spite of such a high DR and film uniformity possessed by the friction transferred film and what could be the possible reason for such a high electrical anisotropy ($\mu_{\parallel}/\mu_{\perp}$). It has been discussed previously

that μ of the PBTTT-C14 stringently depends on several factors such as nature of the self-assembled monolayer, annealing temperature, and surface roughness of the SiO_2 interface. Effect of SiO_2 roughness can be ignored here since the same substrates were used for above discussed FTM-based OFETs, where the observed value of μ was considerably high. This lower value of μ can be attributed to the absence of SAM layer at the interface and the similar results were also observed in the case of oriented films of PBTTT-C12 by mechanical rubbing as reported by Biniek et al.[46]. On the other hand, the value of $\mu_{\parallel}/\mu_{\perp}$ depends on the nature of the confirmation that macromolecules adopt during orientation. This is well-known that the use of shear forces in methods like friction transfer and mechanical rubbing induce *face-on* confirmations [25] which can be understood by the perusal of the spectra of the PBTTT-C14 in both the cases of FTM and friction transfer (Figure 4 & 6). Pronounced shoulders in the spectra of friction transferred films are attributed to the conformational changes of the macromolecules that is *face-on* here. Hosokawa et al. have also reported such spectral difference arises due to conformational changes and with similarly very high $\mu_{\parallel}/\mu_{\perp}$ value [45].

In spite huge material wastage, difficulty in multilayer coating and preparation of non-oriented isotropic films, spin-coating has been most commonly used for fabrication of thin films towards their application in a variety of organic electronic devices due to its simplicity. Need for uniform and pinhole-free thin films has been advocated for the fabrication of high performance devices but there are fewer reports about the uniformity of fabricated spin-coated films. In order to investigate the thickness uniformity of spin-coated films, we utilized 2D positional profiling of thickness distribution in the spin coated thin films PBTTT-C14 on the glass substrate (1 cm × 2.5 cm). Although spin-coated films appear to be uniform by naked eye (**Figure 7**), mapped thickness profile shown the in Figure 7 (a-c) reveals that actually films are not that much uniform and films in the center region are thinner as compared to that of peripheral regions. In Figure 7 (a), the projection of the sample's thickness profile in horizontal plane (pink closed circles) represents the location of the corresponding point-area being mapped

on the sample. Partly magnified image of Figure 7 (a), shows the side-by-side arrangement of 25 point areas (with diameter = 0.2 mm) in 5mm, in this manner the whole sample was probed point by point and the corresponding discrete thicknesses (Figure 7(b)) were integrated to realize the trend of thickness variation in the sample (Figure 7 (c)). Thickness was found to increase gradually from the center (about 15 nm) and reaches up 25 nm in the periphery. Integrating the complete mapped area of 1 cm × 2.2 cm gives an average thickness of 21.10 nm (± 9.749%).

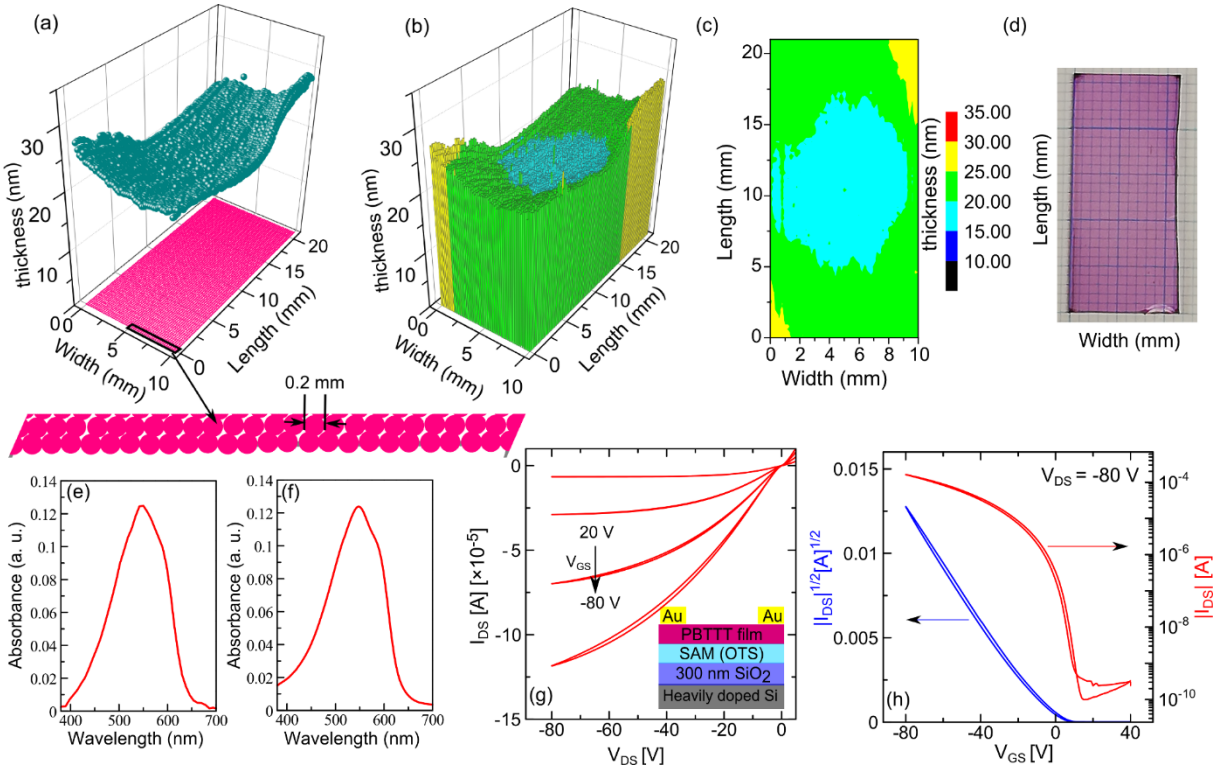

Figure 7. 2D positional profile of thickness (a-c) in the spin-coated thin films of PBTTT-C14 (d). (a) Arrangement of point area (with diameter = 0.2 mm) on the sample and corresponding thickness. Discrete (b) and integrated (c) thickness profile of the spin-coated film (d). Electronic absorption spectra of the films obtained through the mapping system (near center)(e) and conventional spectrophotometer (f). Output curve (g) and transfer characteristics (h) for OFETs fabricated using spin-coated films. Inset in (g) is the device architecture of the OFET, where OTS treated substrates were utilized and samples were annealed similarly to the earlier cases.

This further suggests that at laboratory level small area spin coating might be good but for large area application, it is not that much suitable. Electronic absorption spectra were taken

at single point (near center) by the mapping system (Figure 7(e)) and conventional spectrophotometer (Figure 7(f)), position of peak -absorbance and vibronic features are almost the same. OFETs fabricated using spin-coated PBTTT-C14 in the device architecture as shown in the inset of Figure 7(g) exhibited typical p-type FET behavior. Analysis of transfer characteristic of this OFET shown in Figure 7(h) exhibited average μ of 0.051 $cm^2/V{\cdot}s$ with good ON/OFF ratio of 10^6. Slightly hampered mobility in the case of spin-coated films as compared to that of FTM could be attributed to lack of orientation hampering the charge transport. Therefore, it can be seen that positional scanning can also be used for the optimization of spin-coating conditions in order to fabricate uniform and homogenous thin films before their utilization for other applications like solar cells and light emitting diodes fabricated over relatively large areas.

After successful verification of usefulness of 2D positional mapping system for PBTTT-C14 thin films fabricated by three different method, it was realized to demonstrate its versatility on other SCPs too. To accomplish this, another SCP of thiophene family poly(3,3‴-didodecyl-quaterthiophene) (PQT-C12) was selected, its oriented thin films were fabricated by ribbon-shaped FTM followed analysis of orientation and thickness profile by 2D positional mapping system. Observed results obtained by two independent systems as shown in **Figure S3**, clearly reveals that spectral nature and optical anisotropy measured at one point by the mapping system is almost similar to that measured by conventional spectrophotometer validating the accuracy of the results obtained by the mapping technique. A very small deviation in the DR measured by mapping system (23.0) and conventional spectrophotometer (22.4) is attributed to the fact that former represents the data from a single point (3.14×10^{-2} mm^2), while the latter one represents the average value for the area covered by the incident beam ($\approx$10 mm^2). Interestingly, when multiple DR mapped for equivalent area ($\approx$10 mm^2) were averaged, it was estimated to 23.1, matching well with that obtained through conventional spectrophotometer.

Taking the advantage of point-by-point scanning done at a regular interval of 0.2 mm in both length and width direction led to profiling of thickness and molecular orientation of entire large area films. The obtained results were combined together to visualize the microstructural distribution in terms of thickness and orientation for the whole specimen under investigation. Results of 2D positional mapping of thickness and molecular orientation for 1 cm × 1 cm samples of PQT-C12 thin films prepared taken from three different locations is shown in **Figure S4**. Quality of the thin films in terms of distribution of the film uniformity and molecular orientation plays an important role in deciding the performance of devices in arrays of logic gates with channel length typically varing between 5-50 μm. Therefore, such a positional mapping of molecular orientation and film homogeneity can be extremely useful to decide the optimum place in ribbon-shaped FTM to be stamped for the fabrication of high performance devices. Encouraged by the results of 2D positional mapping pertaining to high molecular orienation in the far-end region, bottom-gated top-contact OFETs were fabricated from far-end films exhibiting high uniformity and high DR to investigate the charge transport anisotropy. Electrical and optical characteristics of all kinds of thin films utilized are summerized in **Table 1**.

Table 1. Electrical and optical characteristics of the various thin films. To fabricate OFETs PBTTT-C14 films were annealled to 160 ℃ for 2 min and PQT-C12 films were annealed to 80 ℃ for 10 min and μ was extrected by analysing eight devices of each type.

Channel feature of the OFET	$\mu_{average}$ ($\mu_{maximum}$) ($cm^2V^{-1}s^{-1}$)		**DR**
	$\mu_{\parallel}$	$\mu_{\perp}$	
PBTTT-C14 (FTM-far region)	0.12 (0.16)	0.042 (0.046)	2 (± 9.5%)
PBTTT-C14 (Friction Transfer)	0.018 (0.021)	9.8×10^{-6} (1.2×10^{-5})	8.2 (± 7.2%)
PBTTT-C14 (Spin-coat)	0.051 (0.06)		
PQT-C12 (FTM-far region)	0.26 (0.30)	1.6×10^{-3} (1.8×10^{-3})	18.3 (± 32.0%)

As can be seen from the output curves, OFETs exhibits clear p-type behavior with high output current at the same gate to source voltage (V_{GS}) in the OFETs, where the channel is in || to orientation direction in comparison to ⊥ as shown in the **Figure S5**. This is a clear indication of charge transport anisotropy and is attributed to the high DR values exhibited by PQT-C12 far end FTM films. Electrical parameters like μ and ON/OFF ratio were estimated from the transfer curve shown in **Figure S5(d)**. Extracted average $\mu_{||}$ and $\mu_{\perp}$ direction were found to be 0.17 $cm^2/V{\cdot}s$ and 4.4 $\times 10^{-2}$ $cm^2/V{\cdot}s$, respectively, for as-cast FTM films. The high ON/OFF ratio of $\sim 10^7$ for || OFETs in comparison to the ⊥ OFETs is attributed to the higher I_{on} in || direction. Upon mild heaing of the films at 80℃ for 10 min, $\mu_{||}$ improved the up to 0.26 $cm^2/V{\cdot}s$, which could be attributed to the promotion of higher extent of molecular self-assembly or removal of the interstitial solvents in the film.

3. Conclusion: 2D positional mapping system has been developed, which is capable of successful profiling of not only the film uniformity (thickness distribution) but also the molecular orientation for large area thin films. Proposed mapping system has been successfully demonstrated its applicability using oriented and non-oriented thin films of PBTTT-C14 prepared by different methods like ribbon-shaped FTM, friction transfer and spin coating, respectively. In spite of high uniformity and molecular orientation in the friction transferred thin film of PBTTT-C14, their utilization for OFET fabrication led to hampered mobility of 0.02 $cm^2/V{\cdot}s$. This was explained by the lack of surface treatment and nature of molecular orientation, where former was found to be the dominant factor for hampered charge transport. Spin-coated thin films of PBTTT-C14 subjected to 2D positional profiling of the film uniformity revealed that films are still non-uniform and there was a gradual increase in the thickness from center to the periphery of the substrate. Almost similar results for molecular orientation obtained from polarized absorption spectral mapping of PQT-C12 films measured by the mapping system and conventional spectrophotometer validates the optimal performance

of the designed mapping system. Utilization of highly oriented and uniform thin film of PQT-C12 from the far-end region of ribbon-shaped FTM as evidenced by the mapping system led to the observation of hole mobility 0.26 $cm^2/V{\cdot}s$ for OFETs fabricated with parallel oriented films. This observed mobility is amongst the best-reported values for this material without annealing at the high temperature (above liquid crystalline temperature). This 2D positional profiling system can also be further improved to map the variations in electronic properties of the materials from point to point to prove the differential performances in devices like OFETs, solar cells and light emitting diodes. Utilizing this setup, in-situ investigation of molecular orientation during the solvent evaporation is also under investigation and will be reported later.

4. Experimental Section

4.1 Materials and methods: PBTTT-C14, dehydrated chloroform, 1,2-dichlorobenzene, octadecyltrichlorosilane (OTS) and 1-octadecene were purchased from Sigma Aldrich. Ribbon-shaped floating films were prepared by placing one drop (~15 μL) of 1% (w/w) PBTTT-C14 dissolved in hot chloroform on the liquid substrate (mixture of ethylene glycol and glycerol in the ratio 3:1, heated at temperature ~ 55 ℃) and the film growth was guided with a custom made slider as schematically shown in the **Figure 1** [31]. Since ribbon-shaped FTM provide large area thin films (> 2 cm × 15 cm), films from different locations were stamped on glass substrates of size 2.5 cm × 1 cm. Area of the film coated on substrates was characterized by 2D positional mapping technique being reported in detail. Thin films of PBTTT-C14 were also prepared by friction transfer technique from its pellet as per the method reported earlier [44]. Thin films by this method were prepared at 75 ℃ with the constant speed of 50 mm/min and a fixed load of 30 Kgf/cm^2. To spin-coat, PBTTT-C14 was dissolved in 1,2-dichlorobenzene with concentrations of 0.25% (w/w) and the solution was spun at 1500 rpm for 120 s on the glass

substrate (2.5 cm × 1 cm). The bottom-gated top-contact OFETs were fabricated on SiO_2 substrate (for details regarding device fabrication, please see-supporting information).

4.2. 2D Positional Mapping Set-up: Incorporation of single beam–multi channel detector system, fine X-Y stage controller and polarizer in the set-up allows us to record the polarized electronic absorption spectrum of the sample at desired locations, which has been schematically illustrated in Figure 2. Photonic multi-channel analyzer (PMA), (C7473-36, Hamamatsu Photonics, Japan) is an important part of this system, which is consisted of a Czerny-Turner type spectrograph and thermoelectric-cooling type back-thinned charge-coupled device (BT-CCD) photodetectors with electronic shutter function. To realize multichannel spectroscopy, an array of 1024 photosensitive BT-CCDs are used in this PMA. The diffraction grating and the multi-channel detector rigidly fixed to get reproducibility in photodetection. The shutter connected to the photodetector unit was externally controlled by connecting a digital function generator (DF1906, NF Corporation, Japan). Multichannel spectral detection by the PMA has been schematically shown in **Figure S6.** A halogen lamp (Megalight 100, Schott, IBE SMT Equipment, Magnolia) coupled with optical fiber and focus lens was used as illumination source. The illumination bandwidth of the halogen lamp covers the wavelength region from 450 nm to 900 nm. For 2D positional mapping, sample stage (Stepping motor-drive SGSP stage/TSDM series, Sigma Koki, Japan) was set in the horizontal plane (X-Y plane), perpendicular to the axis of aligned light source and detector. Sample stage was fixed at 10 cm distance from the focus lens to obtain optimum illumination intensity along with the ease of handling and its motion in X-Y plane was controlled through 2D stage controller (Mark-12, Sigma Koki, Japan) [47]. The stage was interfaced with the stage controller through 2-axis micro-driver. To measure the orientation behavior quantitatively, a polarizer (polarizing film fixed on a rotation motorized stage, SGSP-40YAW, Tamagawa Seiki, Japan) was placed between the light source and the sample stage. The polarizer was rotated with the help of a 4-axis stage controller (SHOT-

304GS: 4 axes, Sigma Koki Co., Ltd., Japan) coupled with controller pad (CJ-200, Sigma Koki Co., Ltd., Japan). Illumination beam coming from the halogen lamp with beam width of 5 mm was vertically incident on the sample. Transmitted beam through the sample was collected by the aligned optical fiber connected to PMA. The collected beam was collimated and dispersed in constituent wavelengths by the spectrograph. The dispersed optical signal was received in the multichannel photodetector. To integrate the photodetectors' output and analyze the absorption spectra, PMA was interfaced with a computer. Five consecutive absorbance data were averaged to increase the signal to noise ratio of the absorption spectrum and measured spectra at each point were further integrated. In order to have a precise mapping of film homogeneity and orientation distribution, the gap between two measuring points and their area should be as minimum as possible. The effective light receiving area of the fiber of the PMA has a diameter of 1 mm, which limits the least possible area to be scanned, to a diameter of 1 mm. In the present setup, a mask of diameter in the range of 0.1 mm - 0.9 mm was incorporated to control the light receiving area. Parameters like speed of the sample stage and signal detection rate of the photodetector are important, which should be tuned to increase the resolution of the measurement. In our present system, it was possible to vary the speed of sample stage between 1 mm/s to 10 mm/s while rate of signal detection was controlled by tuning the shutter opening frequency (between 0.1 mHz to 2 MHz), which was controlled by the digital function generator. In this work, measurement parameters like mask diameter of 0.2 mm, stage speed of 1 mm/s and shutter frequency of 5 Hz with 10% duty cycle were found to be optimum (for detail regarding the optimization of these parameters, see the supporting information).

Acknowledgements: Authors would like to thank and acknowledge late Prof. Wataru Takashima for the planning, conceptualization and design of the proposed 2D positional mapping system.

References

[1] T. Someya, T. Sekitani, S. Iba, Y. Kato, H. Kawaguchi, T. Sakurai, Paper-like electronic displays: Large-area rubber-stamped plastic sheets of electronics and microencapsulated electrophoretic inks, PNAS. 98 (2004) 4835–4840. doi:10.1073/pnas.091588098.

[2] K. Myny, E. Van Veenendaal, G.H. Gelinck, J. Genoe, W. Dehaene, P. Heremans, An 8-bit, 40-instructions-per-second organic microprocessor on plastic foil, IEEE J. Solid-State Circuits. 47 (2012) 284–291. doi:10.1109/JSSC.2011.2170635.

[3] H.H. Chou, A. Nguyen, A. Chortos, J.W.F. To, C. Lu, J. Mei, T. Kurosawa, W.G. Bae, J.B.H. Tok, Z. Bao, A chameleon-inspired stretchable electronic skin with interactive colour changing controlled by tactile sensing, Nat. Commun. 6 (2015). doi:10.1038/ncomms9011.

[4] H. Klauk, Organic thin-film transistors, Chem. Soc. Rev. 39 (2010) 2643. doi:10.1039/b909902f.

[5] K. Tremel, S. Ludwigs, Morphology of P3HT in thin films in relation to optical and electrical properties, Adv. Polym. Sci. 265 (2014) 39–82. doi:10.1007/12_2014_288.

[6] C. Adachi, Third-generation organic electroluminescence materials, Jpn. J. Appl. Phys. 53 (2014) 060101. doi:10.7567/JJAP.53.060101.

[7] T. Berzina, K. Gorshkov, A. Pucci, G. Ruggeri, V. Erokhin, Langmuir–Schaefer films of a polyaniline–gold nanoparticle composite material for applications in organic memristive devices, RSC Adv. 1 (2011) 1537. doi:10.1039/c1ra00584g.

[8] K. Gorshkov, T. Berzina, On the Hysteresis Loop of Organic Memristive Device, Bionanoscience. 1 (2011) 198–201. doi:10.1007/s12668-011-0021-6.

[9] S. Lizin, S. Van Passel, E. De Schepper, W. Maes, L. Lutsen, J. Manca, D. Vanderzande, Life cycle analyses of organic photovoltaics: a review, Energy Environ. Sci. 6 (2013) 3136. doi:10.1039/c3ee42653j.

[10] S. Holliday, Y. Li, C.K. Luscombe, Recent advances in high performance donor-acceptor polymers for organic photovoltaics, Prog. Polym. Sci. 70 (2017) 34–51. doi:10.1016/j.progpolymsci.2017.03.003.

[11] K. Bhargava, V. Singh, High-sensitivity organic phototransistors prepared by floating film transfer method, Appl. Phys. Express. 9 (2016) 091601. doi:10.7567/APEX.9.091601.

[12] E.J.W. Crossland, K. Tremel, F. Fischer, K. Rahimi, G. Reiter, U. Steiner, S. Ludwigs, Anisotropic charge transport in spherulitic Poly(3-hexylthiophene) films, Adv. Mater. 24 (2012) 839–844. doi:10.1002/adma.201104284.

[13] M. Pandey, S. Nagamatsu, W. Takashima, S.S. Pandey, S. Hayase, Interplay of Orientation and Blending: Synergistic Enhancement of Field Effect Mobility in Thiophene-Based Conjugated Polymers, J. Phys. Chem. C. 121 (2017) 11184–11193. doi:10.1021/acs.jpcc.7b03416.

[14] K. Bhargava, V. Singh, High-sensitivity organic phototransistors prepared by floating film transfer method, Appl. Phys. Express. 9 (2016) 091601. doi:10.7567/APEX.9.091601.

[15] S.R. Forrest, The path to ubiquitous and low-cost organic electronic appliances on plastic, Nature. 428 (2004) 911–918. doi:10.1038/nature02498.

[16] Y. Diao, B.C.K. Tee, G. Giri, J. Xu, D.H. Kim, H.A. Becerril, R.M. Stoltenberg, T.H. Lee, G. Xue, S.C.B. Mannsfeld, Z. Bao, Solution coating of large-area organic semiconductor thin films with aligned single-crystalline domains, Nat. Mater. 12

(2013) 665–671. doi:10.1038/nmat3650.
[17] A.L. Briseno, R.J. Tseng, M.M. Ling, E.H.L. Falcao, Y. Yang, F. Wudl, Z. Bao, High-performance organic single-crystal transistors on flexible substrates, Adv. Mater. 18 (2006) 2320–2324. doi:10.1002/adma.200600634.
[18] S. Galindo, A. Tamayo, F. Leonardi, M. Mas-Torrent, Control of Polymorphism and Morphology in Solution Sheared Organic Field-Effect Transistors, Adv. Funct. Mater. 27 (2017) 1700526. doi:10.1002/adfm.201700526.
[19] I. Kang, H. Yun, D.S. Chung, S. Kwon, Y. Kim, Record High Hole Mobility in Polymer Semiconductors via Side-Chain Engineering Record High Hole Mobility in Polymer Semiconductors via Side-Chain Engineering, J. Am. Chem. Soc. 135 (2013) 14896–14899. doi:10.1021/ja405112s.
[20] H. Tseng, H. Phan, C. Luo, M. Wang, L.A. Perez, S.N. Patel, L. Ying, E.J. Kramer, T. Nguyen, G.C. Bazan, A.J. Heeger, High-Mobility Field-Effect Transistors Fabricated with Macroscopic Aligned Semiconducting Polymers, (2014) 2993–2998. doi:10.1002/adma.201305084.
[21] I. Mcculloch, M. Heeney, M.L. Chabinyc, D. Delongchamp, R.J. Kline, M. Cölle, W. Duffy, D. Fischer, D. Gundlach, B. Hamadani, R. Hamilton, L. Richter, A. Salleo, M. Shkunov, D. Sparrowe, S. Tierney, W. Zhang, Semiconducting thienothiophene copolymers: Design, synthesis, morphology, and performance in thin-film Organic transistors, Adv. Mater. 21 (2009) 1091–1109. doi:10.1002/adma.200801650.
[22] H. Sirringhaus, P.J. Brown, R.H. Friend, M.M. Nielsen, K. Bechgaard, B.M.W. Langeveld-Voss, A.J.H. Spiering, R.A.J. Janssen, E.W. Meijer, P. Herwig, D.M. De Leeuw, Two-dimensional charge transport in self-organized, high-mobility conjugated polymers, Nature. 401 (1999) 685–688. doi:10.1038/44359.
[23] M. Pandey, S.S. Pandey, S. Nagamatsu, S. Hayase, W. Takashima, Solvent driven performance in thin floating-films of PBTTT for organic field effect transistor: Role of macroscopic orientation, Org. Electron. Physics, Mater. Appl. 43 (2017) 240–246. doi:10.1016/j.orgel.2017.01.031.
[24] M. Pandey, A. Gowda, S. Nagamatsu, S. Kumar, W. Takashima, S. Hayase, S.S. Pandey, Rapid Formation and Macroscopic Self-Assembly of Liquid-Crystalline, High-Mobility, Semiconducting Thienothiophene, Adv. Mater. Interfaces. 5 (2018) 1700875. doi:10.1002/admi.201700875.
[25] M. Brinkmann, L. Hartmann, L. Biniek, K. Tremel, N. Kayunkid, Orienting semi-conducting pi-conjugated polymers, Macromol. Rapid Commun. 35 (2014) 9–26. doi:10.1002/marc.201300712.
[26] D. Khim, A. Luzio, G.E. Bonacchini, G. Pace, M.-J. Lee, Y.-Y. Noh, M. Caironi, Uniaxial Alignment of Conjugated Polymer Films for High-Performance Organic Field-Effect Transistors, Adv. Mater. 1705463 (2018) 1705463. doi:10.1002/adma.201705463.
[27] T. Morita, V. Singh, S. Nagamatsu, S. Oku, W. Takashima, K. Kaneto, Enhancement of transport characteristics in poly(3-hexylthiophene) films deposited with floating film transfer method, Appl. Phys. Express. 2 (2009) 12–15. doi:10.1143/APEX.2.111502.
[28] M. Pandey, S. Sadakata, S. Nagamatsu, S.S. Pandey, S. Hayase, W. Takashima, Layer-by-layer coating of oriented conjugated polymer films towards anisotropic electronics, Synth. Met. 227 (2017) 29–36. doi:10.1016/j.synthmet.2017.02.018.
[29] S. Kang, J.B. Pyo, T.S. Kim, Layer-by-Layer Assembly of Free-Standing Nanofilms by Controlled Rolling, Langmuir. 34 (2018) 5831–5836. doi:10.1021/acs.langmuir.8b01063.
[30] T. Morita, V. Singh, S. Oku, S. Nagamatsu, W. Takashima, S. Hayase, K. Kaneto, Ambipolar transport in bilayer organic field-effect transistor based on poly(3-hexylthiophene) and fullerene derivatives, Jpn. J. Appl. Phys. 49 (2010) 0416011–

0416015. doi:10.1143/JJAP.49.041601.
[31] A.S.M. Tripathi, M. Pandey, S. Sadakata, S. Nagamatsu, W. Takashima, S. Hayase, S.S. Pandey, Anisotropic charge transport in highly oriented films of semiconducting polymer prepared by ribbon-shaped floating film, Appl. Phys. Lett. 112 (2018) 123301. doi:10.1063/1.5000566.
[32] A. Tripathi, M. Pandey, S. Nagamatsu, S.S. Pandey, S. Hayase, W. Takashima, Casting Control of Floating-films into Ribbon-shape Structure by modified Dynamic FTM, J. Phys. Conf. Ser. 924 (2017) 012014. doi:10.1088/1742-6596/924/1/012014.
[33] M. Pandey, S.S. Pandey, S. Nagamatsu, S. Hayase, W. Takashima, Controlling Factors for Orientation of Conjugated Polymer Films in Dynamic Floating-Film Transfer Method, J. Nanosci. Nanotechnol. 17 (2017) 1915–1922. doi:doi:10.1166/jnn.2017.12816.
[34] M. Pandey, S. Nagamatsu, S.S. Pandey, S. Hayase, W. Takashima, Orientation Characteristics of Non-regiocontrolled Poly (3-hexyl-thiophene) Film by FTM on Various Liquid Substrates, J. Phys. Conf. Ser. 704 (2016) 012005. doi:10.1088/1742-6596/704/1/012005.
[35] M. Pandey, S.S. Pandey, S. Nagamatsu, S. Hayase, W. Takashima, Influence of backbone structure on orientation of conjugated polymers in the dynamic casting of thin floating-films, Thin Solid Films. 619 (2016) 125–130. doi:10.1016/j.tsf.2016.11.015.
[36] M.M. Nahid, E. Gann, L. Thomsen, C.R. McNeill, NEXAFS spectroscopy of conjugated polymers, Eur. Polym. J. 81 (2016) 532–554. doi:10.1016/j.eurpolymj.2016.01.017.
[37] X. Zhang, L.J. Richter, D.M. Delongchamp, R.J. Kline, M.R. Hammond, I. McCulloch, M. Heeney, R.S. Ashraf, J.N. Smith, T.D. Anthopoulos, B. Schroeder, Y.H. Geerts, D.A. Fischer, M.F. Toney, Molecular packing of high-mobility diketo pyrrolo-pyrrole polymer semiconductors with branched alkyl side chains, J. Am. Chem. Soc. 133 (2011) 15073–15084. doi:10.1021/ja204515s.
[38] M.L. Chabinyc, X-ray scattering from films of semiconducting polymers, Polym. Rev. 48 (2008) 463–492. doi:10.1080/15583720802231734.
[39] M.S. Park, A. Aiyar, J.O. Park, E. Reichmanis, M. Srinivasarao, Solvent evaporation induced liquid crystalline phase in poly(3-hexylthiophene), J. Am. Chem. Soc. 133 (2011) 7244–7247. doi:10.1021/ja110060m.
[40] F.C. Spano, Modeling disorder in polymer aggregates: The optical spectroscopy of regioregular poly(3-hexylthiophene) thin films, J. Chem. Phys. 122 (2005) 234701. doi:10.1063/1.1914768.
[41] M.L. Chabinyc, M.F. Toney, R.J. Kline, I. McCulloch, M. Heeney, X-ray scattering study of thin films of poly(2,5-bis(3-alkylthiophen-2-yl)thieno[3,2-b]thiophene)., J. Am. Chem. Soc. 129 (2007) 3226–3237. doi:10.1021/ja0670714.
[42] M.J. Lee, D. Gupta, N. Zhao, M. Heeney, I. Mcculloch, H. Sirringhaus, Anisotropy of charge transport in a uniaxially aligned and chain-extended, high-mobility, conjugated polymer semiconductor, Adv. Funct. Mater. 21 (2011) 932–940. doi:10.1002/adfm.201001781.
[43] J.C. Wittmann, P. Smith, Highly oriented thin films of poly(tetrafluoroethylene) as a substrate for oriented growth of materials, Nature. 352 (1991) 414–417. doi:10.1038/352414a0.
[44] S. Nagamatsu, W. Takashima, K. Kaneto, Y. Yoshida, N. Tanigaki, K. Yase, K. Omote, Backbone arrangement in “friction-transferred” regioregular poly(3-alkylthiophene)s, Macromolecules. 36 (2003) 5252–5257. doi:10.1021/ma025887t.
[45] Y. Hosokawa, M. Misaki, S. Yamamoto, M. Torii, K. Ishida, Y. Ueda, Molecular orientation and anisotropic carrier mobility in poorly soluble polythiophene thin films,

Appl. Phys. Lett. 100 (2012) 203305. doi:10.1063/1.4718424.
[46] L. Biniek, N. Leclerc, T. Heiser, R. Bechara, M. Brinkmann, Large scale alignment and charge transport anisotropy of pBTTT films oriented by high temperature rubbing, Macromolecules. 46 (2013) 4014–4023. doi:10.1021/ma400516d.
[47] SCHOTT MegaLight 100V / MegaLight 200V https://www.schott.com/d/lightingimaging/9355f580-1464-47f7-a766-a05153656863/schott-datasheet-megalight-100v-200v-japanese-18092017.pdf (accessed Aug 15, 2018)

Supporting Information

2D Positional profiling of orientation and thickness uniformity in the semiconducting polymers thin films

Nikita Kumari,[a,*] Atul S. M. Tripathi,[a] Sadakata Shifumi,[a] Manish Pandey,[a] Shuichi Nagamatsu,[b] Shuzi Hayase,[a] Shyam S. Pandey,[a,**]

[a]Division of Green Electronics, Graduate School of Life Science and Systems Engineering, Kyushu Institute of Technology, Wakamatsu, Kitakyushu, 808-0196 Japan

[b]Department of Computer Science and Electronics, Kyushu Institute of Technology, Iizuka, 820-2502 Japan

Corresponding Author
*Nikita Kumari (nikita.jisce@gmail.com)
**Prof. Shyam S. Pandey (shyam@life.kyutech.ac.jp)

A. Device Fabrication Methods

All the OFETs were fabricated in bottom-gated top contact device architecture on highly doped (p++) silicon (Si) wafers with 300 nm thick grown silicon dioxide (SiO_2) as a insulating layer with a capacitance (C_i) of 10 nF/cm^2. The wafers were cleaned with acetone, isopropanol and finally with ultrapure water in ultrasonic bath (5 min each). To remove the residual moisture the wafers were baked at 120 °C for 1 h, in ambient atmosphere. Four types of OFETs were fabricated and for each case the substrate preparation was changed due to various reason explained below. However, the deposition of the electrode and channel dimension remains same in each case. A nickel shadow mask with channel length and width 20 μm and 2 mm respectively was used to pattern the source and drain of electrodes (gold) by thermal evaporation (rate ~ 1.5 Å/s) at a pressure of ~ 10^{-6} Torr.

1. Substrate preparation for PBTTT deposited by FTM / Spin-Coating: Since PBTTT-C14 show liquid crystalline (LC) temperature at around ~140 °C, where side chains melts and

polymeric backbones recrystallize to form big ordered domains that is terrace phase. Moreover, this phenomenon is more surface specific, i.e, hydrophobicity of the dielectric interface as explained by Chabinyc et al. [1]. To carry the annealing process above 150 ℃, we preferred to treat SiO_2 surface with self-assembled monolayer (SAM) of octadecyltrichlorosilane (OTS).

The Si/SiO_2 were placed inside a closed glass bottle containing a 10×10^{-3} M solution of OTS in 1-octadecene at 110 ℃ for 2 h followed by washing in a mixture of super-dehydrated chloroform and cyclohexane in an ultrasonic bath for 5 min and then dried at 150 °C for 1 h. The PBTTT-C14 films were casted on the OTS treated surface (stamped from ribbon-shaped FTM film or spun from PBTTT-C14 dissolved in hot 1,2-dichlorobenzene with 0.25% w/w concentration at 1500 rpm) and annealed in argon atmosphere at 160 ℃ for 2 min and slowly cooled down to room temperature.

2. Substrate preparation for PBTTT deposited by friction transfer method: Si/SiO_2 surface was used to coat the oriented thin film of PBTTT-C14 through friction transferred method then annealed in argon atmosphere at 160 ℃ for 2 min and slowly cooled down to room temperature.

3. Substrate preparation for PQT-C12 deposited by FTM: In spite of the fact that PQT-C12 exhibit LC behavior, the FTM films exhibit high level of ordering in the as-cast state and gets disturbed if annealed at LC temperature [2], therefore, to process the films, CYTOP was preferred as a thin coating layer above the SiO_2 surface to increase the hydrophobicity of the surface. CYTOP^{TM}/CT-Solv.180 mixed in 1:3 volume ratio was spun on SiO_2 surface at 3000 rpm for 120 s and then annealed at 150 ℃ for 1 h. The resultant C_i of CYTOP^{TM} coated substrates was measured and found to be 8 nF/cm^2. The FTM film of PQT-C12 was stamped on the substrate followed by washing with methanol to remove the residual liquid substrate stick to the SCP film. The mild annealing was also done at 80 ℃, which was below the glass transition temperature of the CYTOP and LC temperature of the PQT-C12 as well.

B. Optimization of measurement parameters

In 2-dimensional mapping technique, there are three inter-dependent measurement parameters which were tuned for optimum precision in characterization and they are i) speed of the sample stage, ii) mask diameter and iii) shutter operating frequency.

In the mapping system, sample is characterized at successive points by controlled movement of the sample stage. The stage controller provides the speed from 1 to 10 mm/s and. The sample is illuminated continuously but the detector receives the signal discretely. Thus, the least speed (1 mm/s) was found to be adequate for optimum precision.

The remaining two parameters were optimized together, keeping the speed of stage fixed to 1 mm/s. The transmitted light through the sample is received by photonic multi-channel analyzer (PMA) and inside the PMA, a shutter is present above the multi-channel detector which was externally controlled through a function generator by sending a rectangular pulse signal, (**Figure 2)**. Since the sample is mobile, so the ON state of the signal should be such that the PMA can received the transmitted beam through focused point on the sample instantly, without any interference from the neighboring area. To avoid the interference, ON state duration of the rectangular pulse signal was fixed to 20 ms, it is also the lowest limit of exposer time for detector of PMA. Therefore, periodic rectangular pulse signal was generated by the function generator, keeping 20 ms ON time in each cycle to control the shutter operation. Further, the frequency of rectangular pulse signal (shutter operating frequency) was optimized along with the mask diameter. The mask diameter should be fixed in such a way that it can focus a different point area in different duty cycle and avoid the overlapping of the scanned areas. Considering the mechanism of 2D positional mapping system, for optimum characterization throughout the sample, three controlling parameters were correlated by the following expression:

$$\text{Mask diameter} = \frac{\text{Stage speed}}{\text{Shutter operaing frequency}}$$

Mask with different diameter 0.1 to 0.9 mm were used to tune the area of point to be characterized. The selection of mask diameter depends on the sample's expected morphology and desired resolution. Although the least possible mask diameter is suggested for the best resolution but if the sample is expected to have less position dependent variation then the mask diameter can be increased for the ease of experiment. In the present work, following measurement parameters were fixed to obtain the results i.e., stage speed at 1 mm/s, mask diameter of 0.2 mm, and shutter operating frequency of 5 Hz with 10% duty cycle and found adequate for the characterization.

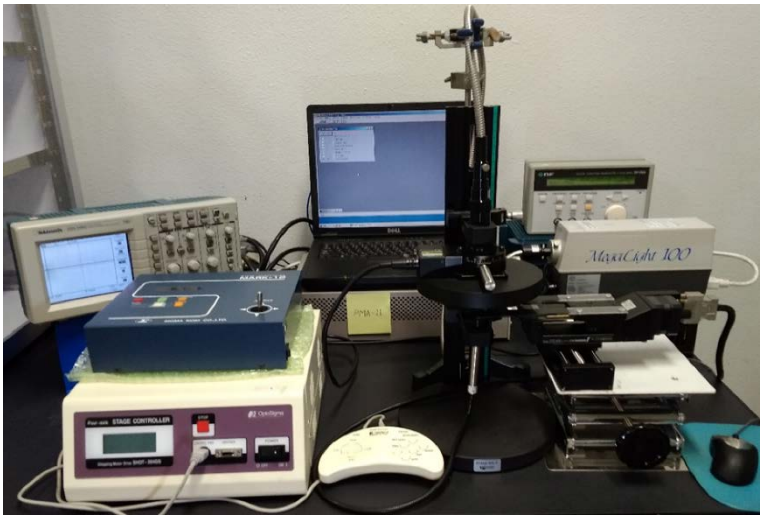

Figure S1. Digital image of the custom-made set up for 2D positional mapping.

C. Correlation between thickness and absorbance

To correlate the distribution of peak-absorbance value of the absorption spectra with the corresponding thickness of the SCP film, average extinction coefficient was calculated. Thickness of the sample film was measured at three different locations (t_1, t_2, t_3), almost homogeneous, and around those points, maximum absorbance values of fifty mapped spectra were averaged out A_1, A_2, A_3. Further they were correlated according to following equations,

Average thickness $$\boldsymbol{t_{av} = \frac{t_1 + t_2 + t_3}{3}}$$ (SEq 1)

Average of peak-absorbance $$\boldsymbol{A_{av} = \frac{A_1 + A_2 + A_3}{3}}$$ (SEq 2)

Correlation between t_{av} and A_{av} (following Beer-Lambert law) [3] $$\boldsymbol{\alpha = \frac{2.303\, A_{av}}{t_{av}}}$$ (SEq 3)

where α is absorption coefficient of the material. Further the distribution in film thickness was interpreted in terms of absorbance distribution.

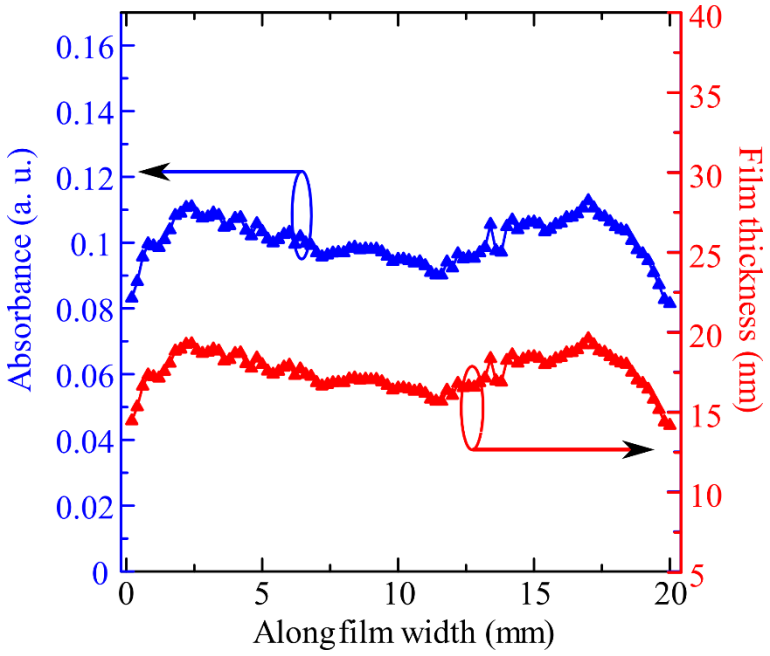

Figure S2. Plot of absorbance profile for far end PBTTT-C14 FTM film along one line, obtained through mapping technique and corresponding thickness.

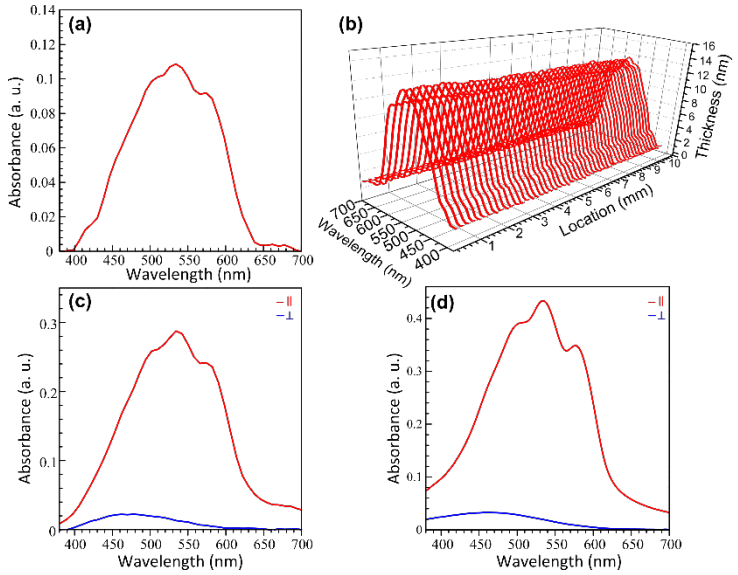

Figure S3. Representative single point absorption spectra (a), and single line absorption spectra (along width, length = 128 mm) along with representative polarized absorption spectra (c), of far-region ribbon-shaped FTM films obtained through mapping technique and polarized absorption spectra obtained through conventional UV-Visible spectrophotometer (d).

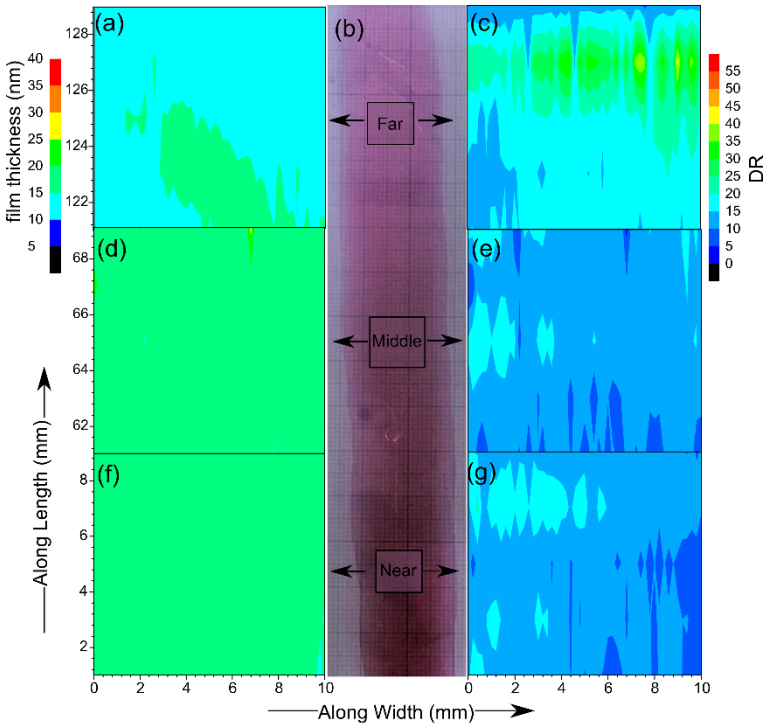

Figure S4. Distribution of thickness (a,d and f) for PQT-C12 films fabricated by ribbon-shaped FTM along with respective DR (c,e and g) probed by the 2D-positional mapping system.

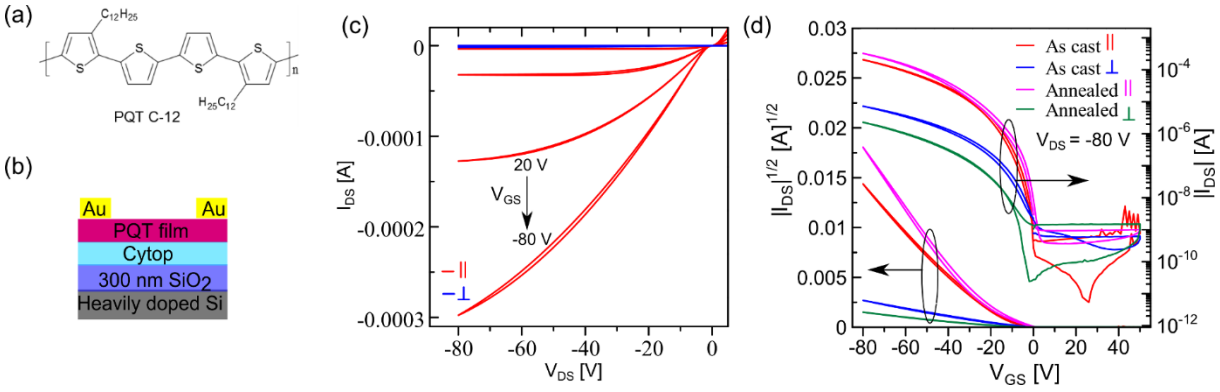

Figure S5. (a) Chemical structure of PQT-C12, (b) schematic of fabricated OFETs, output (c) and transfer (d) characteristics of OFETs, fabricated using PQT-C12 far end FTM films, with channel parallel (||) and perpendicular (⊥) to the orientation direction.

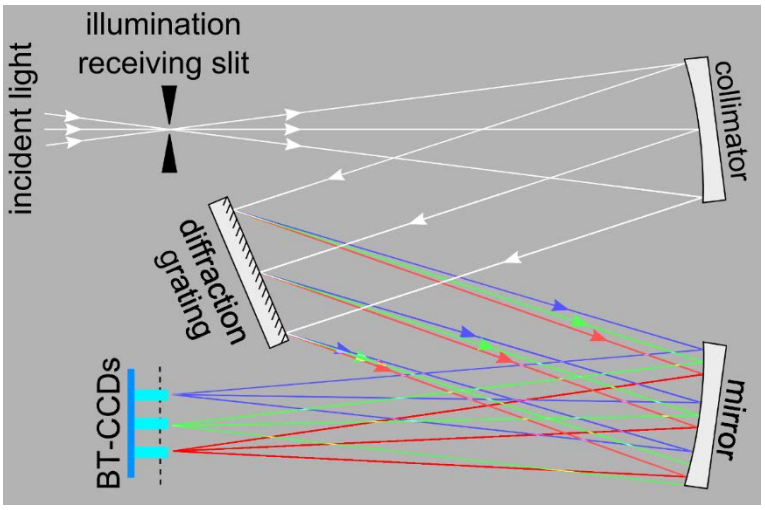

Figure S6. Schematic illustration for working mechanism of spectrograph inside Photonic Multi-channel Analyzer.

References

[1] M.L. Chabinyc, M.F. Toney, R.J. Kline, I. McCulloch, M. Heeney, X-ray scattering study of thin films of poly(2,5-bis(3-alkylthiophen-2-yl)thieno[3,2-b]thiophene)., J. Am. Chem. Soc. 129 (2007) 3226–3237. doi:10.1021/ja0670714.

[2] A.S.M. Tripathi, M. Pandey, S. Sadakata, S. Nagamatsu, W. Takashima, S. Hayase, S.S. Pandey, Anisotropic charge transport in highly oriented films of semiconducting polymer prepared by ribbon-shaped floating film, Appl. Phys. Lett. 112 (2018) 123301. doi:10.1063/1.5000566.

[3] Wikipedia, “Beer-Lambert law,” http://en.wikipedia.org/wiki/ Beer-Lambert_law.